

Relative and absolute neutron-induced fission cross sections of ^{208}Pb , ^{209}Bi , and ^{238}U in the intermediate energy region

V. P. Eismont,¹ A. V. Prokofyev,¹ A. N. Smirnov,¹ K. Elmgren,^{2,*} J. Blomgren,² H. Condé,² J. Nilsson,² N. Olsson,² T. Rönnqvist,³ and E. Tranéus³

¹*V. G. Khlopin Radium Institute, 2nd Murinski av. 28, Saint-Petersburg 194021, Russia*

²*Department of Neutron Research, Uppsala University, Box 535, S-75121 Uppsala, Sweden*

³*Department of Radiation Sciences, Uppsala University, Box 535, S-75121 Uppsala, Sweden*

(Received 27 November 1995)

Measurements of neutron-induced fission cross sections for ^{208}Pb , ^{209}Bi , and ^{238}U have been performed in the 70–160 MeV energy region at the neutron beam facility at the The Svedberg Laboratory in Uppsala using the $^7\text{Li}(p,n)$ reaction as neutron source. The fission fragments were detected by thin-film breakdown counters. The neutron flux was measured relative to the n - p scattering cross section with a proton-recoil spectrometer. The results are compared with calculations and with earlier reported experimental data. [S0556-2813(96)03506-6]

PACS number(s): 25.85.Ec, 24.75.+i

I. INTRODUCTION

Data on neutron-induced fission cross sections are of interest in fundamental nuclear physics (studies of competition between different decay modes of excited nuclei; testing of theoretical nuclear models) as well as for applied nuclear research (transmutation of long-lived nuclear waste; neutron cross section standards) [1–3]. Until recently there are only a few experimental studies of neutron-induced fission cross sections in the energy region above 20 MeV [4–9]. In particular, very few measurements have been made for nuclei lighter than the actinides.

An experimental facility, intended for measurements of neutron and charged-particle induced fission cross sections, was designed using thin-film breakdown counters (TFBC's) for fission fragment detection [10,11]. Preliminary results of $^{209}\text{Bi}(n,f)$ and $^{238}\text{U}(n,f)$ cross section measurements at 135 and 162 MeV were published recently [12].

In the present work, experimental data are given on the $^{208}\text{Pb}(n,f)$, $^{209}\text{Bi}(n,f)$ and $^{238}\text{U}(n,f)$ cross sections in the 70–160 MeV energy region. The results are compared with calculations using the LAHET code [13] as well as with data from measurements reported by other groups.

II. EXPERIMENTAL PROCEDURE

A. The neutron beam

The measurements were performed at the neutron beam facility, using the Gustaf Werner Cyclotron, at the The Svedberg Laboratory, Uppsala [14]. The neutrons were produced by the $^7\text{Li}(p,n)$ reaction in 200–400 mg/cm² thick discs of enriched ^7Li . The intensity of the collimated neutron beam varied in the 10^5 – 10^6 neutrons/s range within a solid angle of 60 μsr . Most of the runs were performed in connection with experiments on n - p scattering [15] and thus it was pos-

sible to obtain the neutron flux relative to the n - p scattering cross section by the use of a proton-recoil spectrometer [14,15]. The n - p scattering data were normalized to the predictions of the phase-shift analyses solution VZ40 [16,17].

An overview of the n - p facility is shown in Fig. 1. The spectrometer consists of a dipole magnet with four drift chambers, and four plastic scintillators. Two of the drift chambers are located in front of the magnet and two behind. The drift chambers are used to determine the emission angle and momentum of the recoiling protons from a thin CH_2 sample by ray-tracing techniques. The four scintillators are used for triggering, particle identification, and neutron time of flight (TOF).

The neutron spectrum consists predominantly of an unresolved doublet, dominated by the ground state transition with an admixture of the transition to the first excited state at 0.43

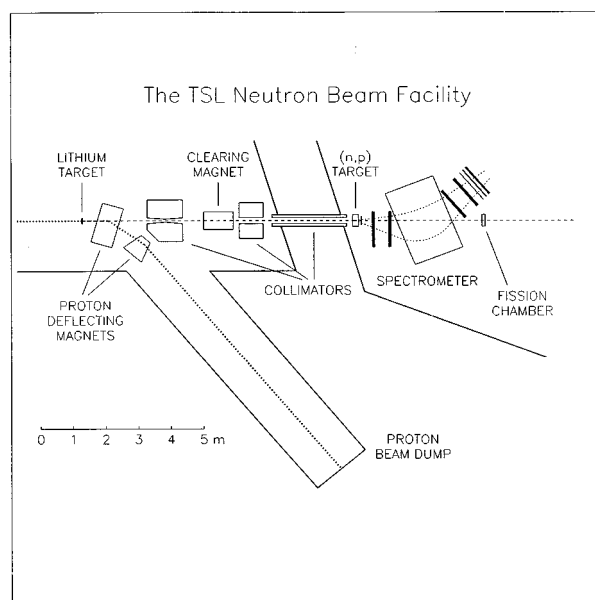


FIG. 1. Overview of the Uppsala neutron beam facility.

*Corresponding author. Fax number: +46 18 183833. Electronic address: klas.elmgren@tsl.uu.se

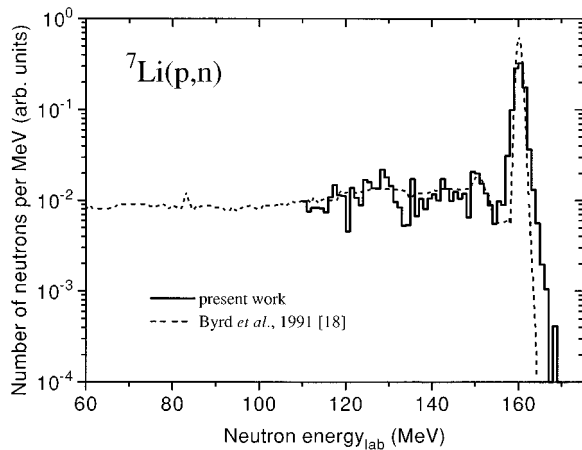


FIG. 2. The neutron spectrum from the ${}^7\text{Li}(p,n)$ reaction at 0° : reconstructed from the n - p experiment (solid line) and measured by Byrd *et al.* [18] for 160 MeV incident proton energy (dashed line). The latter spectrum has been shifted by 2 MeV. The spectra were normalized using the area under the high energy peak.

MeV. In addition, it has a low energy tail, related to highly excited states in the product nucleus. The width of the peak is mainly given by the thickness of the lithium target. The energy resolution of the n - p spectrometer, including the sample, is about 3.0 MeV for 162 MeV neutrons, mainly due to the energy resolution of the proton-recoil spectrometer.

An example of a neutron spectrum reconstructed from n - p scattering data is given in Fig. 2 for the 162 MeV run (here and below the neutron energy corresponds to the high energy peak value in the neutron energy spectrum). A good agreement was found between this spectrum and the one independently measured by Byrd *et al.* [18] at nearly the same proton energy. This shows that neutron scattering in the neutron beam collimator system does not create any significant distortion of the neutron spectrum.

The time structure of the beam (micropulses about 2–4 ns long with a repetition period of about 50–70 ns) and a flight-path length of 12 m made it possible to distinguish high and low energy neutrons using TOF techniques.

The neutron beam profiles are reconstructed from the n - p scattering data. The neutron flux density is uniform within a circular area with a diameter of about 7 cm at the CH_2 sample position which corresponds to a uniform beam with a diameter of 9–10 cm in the fission chamber position.

B. The fission fragment detectors and the fission chambers

The fission reaction rates were measured with thin-film breakdown counters (TFBC's) [10,11] developed at the Khlopin Radium Institute. The TFBC's have low inherent background and they are not sensitive to background from spallation reaction residues which are induced in competition with fission. Good timing properties of the TFBC's allowed the use of TOF techniques to distinguish fissions induced by neutrons in the high energy peak from those in the low energy tail of the neutron energy spectrum. The small thickness of a TFBC (0.3 mm Si) made it possible to place several TFBC's in a close geometry following each other in the neutron beam without any significant influence on the beam characteristics.

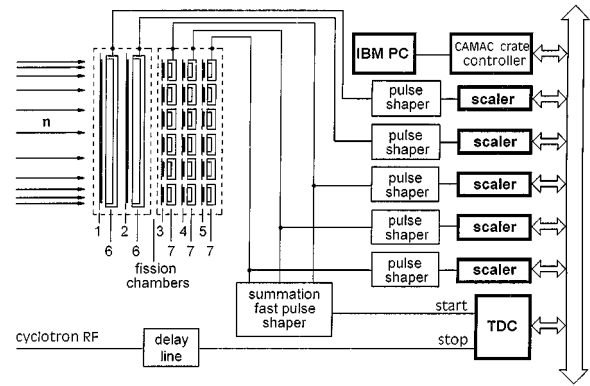


FIG. 3. A schematic drawing of the fission chambers and the electronics. 1 and 3 corresponds to the ${}^{209}\text{Bi}$ samples, 2 and 4 to ${}^{238}\text{U}$, 5 to ${}^{208}\text{Pb}$, 6 to the large area TFBC's and 7 to the mosaic arrangement of TFBC's.

Two fission chambers in an open nonvacuum arrangement, containing fissile samples and TFBC's in a close geometry, were placed perpendicular to the neutron beam direction behind the n - p spectrometer (Fig. 1). A layout of the fission chambers is shown in the left of Fig. 3.

The first chamber contained ${}^{209}\text{Bi}$ and ${}^{238}\text{U}$ samples with large area TFBC's mounted close together like a sandwich to provide maximum solid angle for the fission fragment detection. The timing properties of these large area TFBC's did not allow TOF selection of the fission events. The diameter of the samples and the TFBC's was about 70 mm, so it was possible to place them within the uniform neutron flux density area.

The second chamber was intended for TOF measurements. This chamber contained three independent "mosaic" arrangements, each one consisting of 26 sandwiches. Each sandwich consisted of a fissile sample (either ${}^{208}\text{Pb}$, ${}^{209}\text{Bi}$, or ${}^{238}\text{U}$) and a TFBC with an area of about 1 cm^2 . The time resolution of one TFBC of this size is about 300 ps and about 2 ns for the mosaic detector as a whole.

Figure 4 shows the dependence of the TFBC detection efficiency on the applied voltage for ${}^{252}\text{Cf}$ spontaneous fission fragments from a remote source (long distance geometry) and from a source placed close to a TFBC (sandwich geometry). It can be seen that contrary to the case of a remote source, there is no plateau in the TFBC efficiency curve in the sandwich geometry. Thus, it was necessary to make a

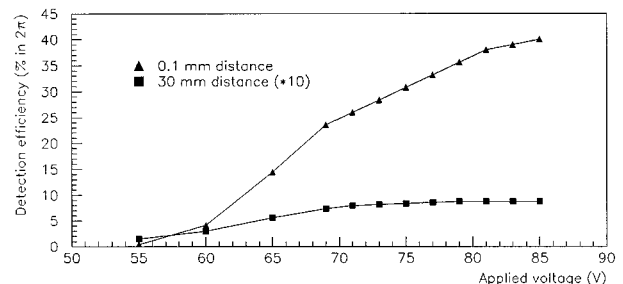


FIG. 4. The TFBC detection efficiency as a function of the applied voltage for a ${}^{252}\text{Cf}$ spontaneous fission fragment source placed at two different positions relative to the TFBC.

careful calibration of the efficiency of the TFBC's in this geometry using a sample containing an amount of ^{252}Cf giving a well-known number of spontaneous fissions per time (see Sec. II C).

C. The fissile samples

Different groups of samples for calibration purposes and for the different TOF and non-TOF measurements were prepared and tested.

(1) The large-area samples (70 mm in diameter) for the non-TOF measurements were prepared by vacuum evaporation onto 0.2 mm thick stainless steel backings using planetary rotation during evaporation to obtain a uniform thickness of the fissile layer. The sample thickness was about 1.6 mg/cm² for ^{209}Bi and 100 μg/cm² for ^{238}U . The weight of the fissile material was determined with an accuracy of about 2%. The variation in thickness over the layer area was less than 2%.

(2) The small-area ^{209}Bi samples intended for the TOF measurements with the mosaic detector had fairly thick layers, about 4 mg/cm², to obtain an acceptable count rate of fission events. The TOF measurements for ^{209}Bi aimed at determining the relative number of fissions induced by high energy neutrons to that by low energy background neutrons. For that reason, it was not necessary to have a high uniformity of the layers or to know the sample weight with high accuracy.

(3) The layer thicknesses of the small-area ^{208}Pb and ^{238}U samples intended for the TOF measurements with the mosaic detectors were about 2.4 mg/cm² and 1.2 mg/cm², respectively. Being without a large-area ^{208}Pb sample, the $^{208}\text{Pb}(n,f)/^{238}\text{U}(n,f)$ cross section ratio was measured using the mosaic detectors only. The weights of the ^{208}Pb and ^{238}U layers in this arrangement were determined with 2% accuracy. The ^{208}Pb samples were 98.7% isotopically pure with an admixture of 1% ^{207}Pb and 0.3% ^{206}Pb .

A possible contamination of natural uranium or thorium in the ^{208}Pb and ^{209}Bi samples was checked by direct alpha-spectroscopy measurements as well as by irradiation with 14 MeV neutrons to register fission events which, at this energy, only can occur in uranium or thorium. The relative abundance of uranium or thorium atoms in the samples did not exceed 10^{-5} .

(4) The samples used in the efficiency calibration of the large- and small-area TFBC's were made of a mixture of natural uranium and several picograms of ^{252}Cf , uniformly spread throughout the sample, giving a well-determined number of spontaneous fissions per second. The layer thicknesses of the calibration samples were chosen to simulate the fission fragment energy losses in the layers of the samples for the different nuclides [10]. The energy spectra of those calibration fission fragments were checked by silicon detectors.

D. The electronics and the data acquisition system

A schematic view of the electronics is shown in Fig. 3. The signal from each large-area TFBC passed through a pulse shaper to a scaler. The signals from the mosaic arrangements were added in a summation fast pulse shaper, and the output started a time-to-digital converter (TDC) with

the cyclotron rf signal as stop. Each mosaic detector signal was recorded in an additional scaler, and this information was used in the analysis to separate the TOF spectra from the different target nuclei.

The data were stored in a computer on an event-by-event basis and could be inspected on line. The data acquisition system involved a beam current signal from the proton beam dump for monitoring purposes. The fission measurement and the n - p scattering runs were synchronized. Special attention was given to the long-term stability of the TOF-peak position. Possible peak shifts due to cyclotron rf system adjustments were automatically corrected for by the data acquisition system.

III. THE DATA PROCESSING

The neutron-induced fission fragment count rate is

$$N_{\text{nf}} = \varepsilon p(A) N_n \int_{E_{\text{min}}}^{E_{\text{max}}} W(E) \sigma_f(E) dE \quad (1)$$

where ε is the detection efficiency in 2π units, $p(A)$ is the number of nuclei per cm² with mass number A in the sample, N_n is the number of neutrons hitting the sample per second, $W(E)$ is the incident neutron spectrum normalized to unity, $\sigma_f(E)$ is the neutron-induced fission cross section, and E is the incident neutron energy.

The detection efficiency obtained from the calibration measurement is

$$\varepsilon = \frac{N_{\text{sf}}}{a_{\text{sf}} S_{\text{TFBC}}}, \quad (2)$$

where N_{sf} is the ^{252}Cf fission fragment count rate, a_{sf} is the spontaneous fission activity of the calibration sample per unit area, and S_{TFBC} is the sensitive area of the TFBC.

In order to obtain the fission cross section at the energy E_0 , corresponding to the peak in the neutron energy spectrum, it is necessary to separate the fissions induced by peak neutrons from those induced by low energy neutrons. For this purpose, all the TOF spectra were decomposed into the two components mentioned above by means of a simple empirical algorithm. In case of the non-TOF measurements with the large ^{209}Bi and ^{238}U samples, a correction was applied for the low energy neutron contribution calculated from the TOF spectrum for the same nuclides.

The correction is

$$k_{\text{low}} = \frac{\sigma_f(E_0) \int_{E_0 - \Delta E}^{E_0 + \Delta E} W(E) dE}{\int_{E_{\text{min}}}^{E_{\text{max}}} W(E) \sigma_f(E) dE}, \quad (3)$$

where $\sigma_f(E_0)$ is the average fission cross section within the neutron energy interval $E_0 \pm \Delta E$.

The final expression for the fission cross section is

$$\sigma_f = \frac{N_{\text{nf}} k_{\text{low}} a_{\text{sf}}}{N_{\text{sf}} p(A) j_n} k_{\text{anis}} k_{\text{LMT}}, \quad (4)$$

where j_n is the the high energy peak neutron flux density in the uniform beam area, k_{anis} and k_{LMT} are corrections for the fission fragment angular anisotropy and the linear momen-

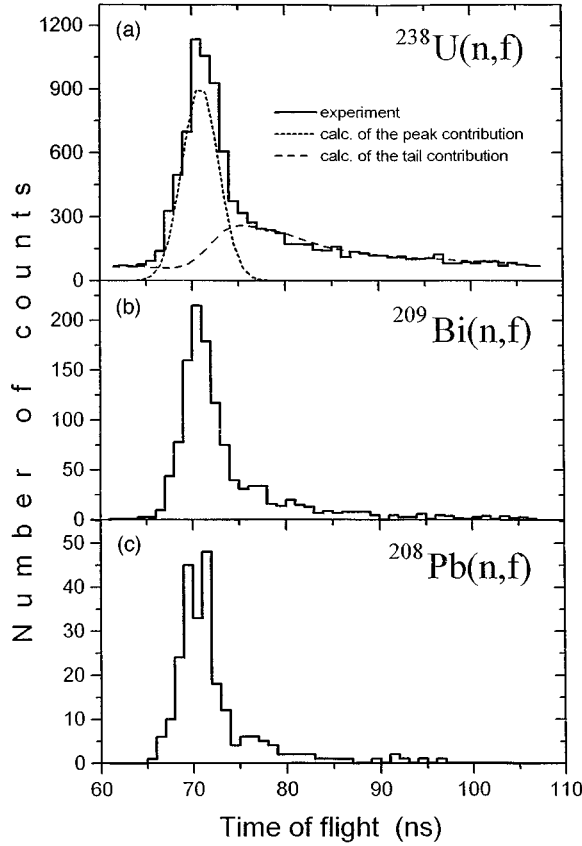


FIG. 5. The TOF spectra of fission events at a neutron energy of 162 MeV. (a) $^{238}\text{U}(n,f)$ (with decomposition), (b) $^{209}\text{Bi}(n,f)$, (c) $^{208}\text{Pb}(n,f)$.

tum transferred by incident neutrons to the fissioning nucleus. Because experimental data on fission anisotropy and linear momentum transfer do not exist for neutrons, the corrections were estimated using proton-induced fission data for the nuclides under study [19–22].

IV. EXPERIMENTAL RESULTS

The measurements were made at neutron energies 73, 96, 135, and 162 MeV. As an example, the TOF spectra of the

$^{238}\text{U}(n,f)$, $^{209}\text{Bi}(n,f)$ and $^{208}\text{Pb}(n,f)$ fission events obtained at 162 MeV are shown in Figs. 5(a)–(c), respectively. The total time resolution was about 4–5 ns (FWHM) with the main contributions coming from the cyclotron pulse width and the inherent time resolution of the mosaic arrangement.

It is seen that the $^{209}\text{Bi}(n,f)$ and $^{208}\text{Pb}(n,f)$ TOF spectra [Figs. 5(b) and (c)] drop rapidly towards lower incident neutron energies due to high fission barriers of the nuclei in this mass region. On the contrary, the $^{238}\text{U}(n,f)$ TOF spectrum [Fig. 5(a)] has a long uniform low energy tail, partly due to a relatively low fission barrier and a fairly weak energy dependence of the fission cross section above 30 MeV. Furthermore, when unfolding the $^{238}\text{U}(n,f)$ TOF spectrum, the contribution of fissions induced by low energy neutrons from previous beam pulses (the so-called “wraparound effect”) has to be taken into account.

In addition to the empirical decomposition algorithm mentioned above, the $^{238}\text{U}(n,f)$ TOF spectrum at 162 MeV was calculated independently using of the $^{238}\text{U}(n,f)$ excitation function shape measured by Lisowski *et al.* [6] and the neutron spectrum for the $^7\text{Li}(p,n)$ reaction measured by Byrd *et al.* [18], taking into account a small difference of the incident proton energy between the work by Byrd *et al.* and the present work. A reasonable agreement was obtained between the calculated and experimentally observed TOF spectrum. Thus, the data presented here are consistent with the data of Lisowski *et al.* and Byrd *et al.* Because the full-energy peak is well separated from the low energy tail in the spectrum measured by Byrd *et al.* (Fig. 2), it was possible to analytically decompose the calculated TOF spectra into the components mentioned above. The result of the analytical decomposition is shown by the dashed line in Fig. 5(a). The k_{low} values obtained for the $^{238}\text{U}(n,f)$ spectrum by the two different algorithms are in good mutual agreement.

The results of the measurements are given in Table I and are shown in Fig. 6 together with previously reported data. The main contributions to the uncertainties of the relative cross sections were due to the uncertainty in the TOF spectrum decomposition procedure. This uncertainty was estimated to be 5% for the $^{238}\text{U}(n,f)$ reaction, 5–6% for the

TABLE I. The relative and absolute neutron-induced fission cross sections for ^{238}U , ^{209}Bi , and ^{208}Pb (mb).

Target nucleus	Neutron energy (MeV)			
	73	96	135 ^a	162
$^{209}\text{Bi}/^{238}\text{U}$	0.0097 ± 0.0009	0.018 ± 0.002	0.028 ± 0.003	0.040 ± 0.004
$^{208}\text{Pb}/^{238}\text{U}$	0.0026 ± 0.0004	0.0053 ± 0.0006		0.016 ± 0.002
^{238}U	—	—	1440 ± 160	1310 ± 120
	1532^b	1430^b	1340^b	1320^b
^{209}Bi	15 ± 1.5^c	25 ± 2^c	40 ± 5	53 ± 5
		38 ± 11^d		
^{208}Pb	3.9 ± 0.5^c	7.5 ± 0.9^c	—	21 ± 3
		21 ± 0.9^e		

^aNo TOF measurements were made at 135 MeV.

^bData measured by Lisowski *et al.* [6].

^cThe absolute value is obtained with the $^{238}\text{U}(n,f)$ cross section measured by Lisowski *et al.* [6] as standard.

^dData measured by Goldanski *et al.* [4] at a neutron energy of 120 ± 40 MeV.

^eData measured by Reut *et al.* [5] with a natural lead target at a neutron energy of 120 ± 40 MeV.

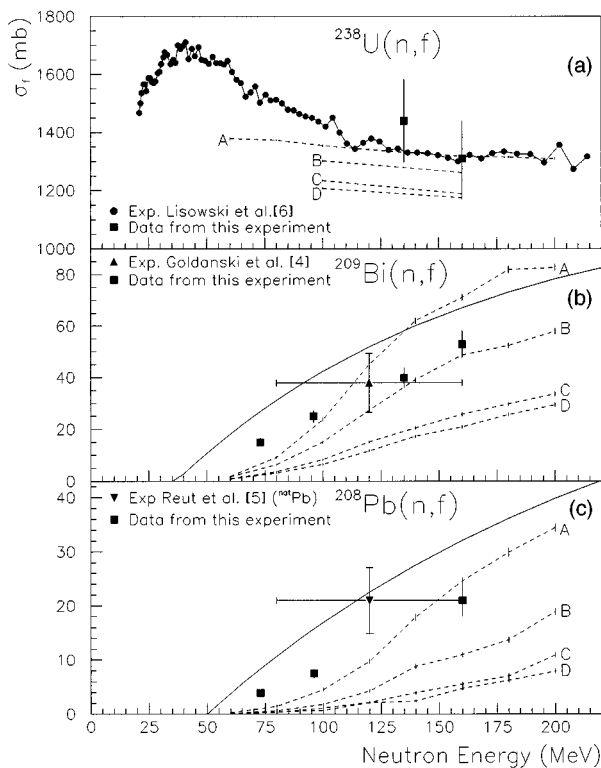


FIG. 6. Neutron-induced fission cross sections: (a) ^{238}U , (b) ^{209}Bi , and (c) ^{208}Pb . The dashed lines represent LAHET code calculations with different options of using one or two nonequilibrium reaction stages, i.e., intranuclear cascade and multistep preequilibrium emission (MPM). Line A corresponds to “MPM turned off” (default option), line B to “pure MPM,” line C to “hybrid MPM,” and line D to “normal MPM.” Error bars near the lines show statistical uncertainties of the Monte Carlo calculations. The solid lines in (b) and (c) show the evaluation by Fukahori and Pearlstein [39] included in the High Energy File of the US Nuclear Data Library (ENDF/B-VI,HE). Note the suppressed zero in (a).

$^{209}\text{Bi}(n,f)$ and 6.5–9 % for the $^{208}\text{Pb}(n,f)$ reactions. The larger uncertainties for the two latter reactions were due to missing information on the excitation functions. The statistical errors were typically 2–2.5 % for ^{209}Bi , 5–10 % for ^{208}Pb , and less than 2% for ^{238}U . The contribution to the systematic errors from the detector calibration was 1–3.5 %, from target thickness 1–3.5 %, from the correction for the anisotropy of fission fragments 2%, and from the estimate of the linear momentum transfer of the incident neutron to the fissioning nucleus 1–2 %. It resulted in a total uncertainty of 12–14 % for the $^{208}\text{Pb}/^{238}\text{U}$ ratio and 9% for the $^{209}\text{Bi}/^{238}\text{U}$ ratio.

Because the TOF techniques were not yet implemented at the 135 MeV measurement, the correction for low energy neutrons was estimated from an interpolation based on the TOF spectrum data obtained in the measurements at the neighboring neutron energies. It resulted in an uncertainty of 12% for the $^{209}\text{Bi}/^{238}\text{U}$ fission cross section ratio at 135 MeV. The ^{208}Pb samples were not present in this experiment.

The absolute fission cross sections were obtained by two different methods.

(a) The neutron flux at 135 and 162 MeV was calculated

from differential $n-p$ scattering cross section measurements made with a magnetic proton recoil spectrometer placed upstream of the fission chambers in the same neutron beam. The errors of the absolute $n-p$ differential scattering cross sections were estimated to be about 5%. Due to uncertainties in the efficiency of the $n-p$ facility (4–5 %) and of the hydrogen content of the CH_2 sample (4–5 %), the total neutron flux uncertainty was estimated to be about 8%. Together with the uncertainties of the relative fission cross sections described above, it gives an absolute cross section uncertainty of 9–13 %.

(b) Because the neutron flux data based on differential $n-p$ scattering cross section measurements were not available at 73 and 96 MeV, the absolute $^{238}\text{U}(n,f)$ cross section measured by Lisowski *et al.* [6] was used as a secondary standard to obtain the $^{209}\text{Bi}(n,f)$ and $^{208}\text{Pb}(n,f)$ cross sections at those neutron energies. The $^{238}\text{U}(n,f)$ data by Lisowski *et al.* were fitted by a polynomial to obtain data at the proper energies. The uncertainties in the $^{238}\text{U}(n,f)$ cross section reference data by Lisowski *et al.* are not included in the uncertainties of the fission cross sections given in Table I.

V. THEORETICAL CALCULATIONS

The $^{238}\text{U}(n,f)$ and $^{209}\text{Bi}(n,f)$ cross sections were calculated with the LAHET code [13,23] using different options and parameters. Results of the calculations were partly given in our previous work [24]. LAHET is a Monte Carlo code for transport and interaction calculations for nucleons and other light particles in complex geometries. It might also be used without particle transport to calculate particle production cross sections. The code includes the Bertini [25] and ISABEL [26,27] (which itself is derived from the VEGAS INC [28]) intranuclear cascade (INC) models, the multistage multistep preequilibrium exciton (MPM) model and several options of the level-density parametrization. Two models are included for fission induced by high energy interactions, the ORNL [29] model and the Rutherford Appelton Laboratory (RAL) [30] model. For the fission models, the evaporation model of Dresner [31] is employed.

The LAHET code calculations were done as follows. The Bertini INC model and the RAL fission model options have been used in all calculations. The subsequent deexcitation of the residual nucleus following the INC interaction may optionally employ a MPM model. If the preequilibrium model is used three optional modes can follow. The MPM continues from the final state of the INC (normal MPM) or the INC is used only to determine that an interaction has occurred (pure MPM) or a random selection is made of one of the first modes at each collision with a certain given probability function (hybrid MPM). Furthermore, three different options are available for the choice of level-density parameter. Those are the level-density model by Gilbert-Cameron-Cook-Ignatyuk [32–35] (default option used in the present calculations), the original HETC level-density formulation and the Jülich mass-dependent parametrization [36] of the level density.

VI. DISCUSSION

A. The $^{238}\text{U}(n,f)$ cross section

The experimental data obtained at two different neutron energies, 135 and 162 MeV, for the $^{238}\text{U}(n,f)$ cross section

are given in Table I and shown in Fig. 6(a). They agree with recent experimental results by Lisowski *et al.* [6]. Arthur and Young [37] calculated the $^{238}\text{U}(n,f)$ cross section for neutron energies up to 100 MeV using the preequilibrium statistical model code GNASH. The results were 25–30 % higher near 100 MeV than the experimental data by Lisowski *et al.*

The $^{238}\text{U}(n,f)$ cross sections calculated with the LAHET code are shown in Fig. 6(a) by dashed lines. Line *A* corresponds to “MPM turned off,” line *B* to “pure MPM,” line *C* to “hybrid MPM,” and line *D* to “normal MPM.” It is seen that the calculated fission cross sections vary within about 10% for different parameter sets. The calculations are in a good agreement with available experimental data for incident neutron energies above about 100 MeV. As pointed out by Prael [38], the discrepancy at lower energies may largely be due to the fact that the nonelastic cross sections calculated with the LAHET code do not describe the experimental data well.

B. The $^{209}\text{Bi}(n,f)$ cross section

The present experimental data on the $^{209}\text{Bi}(n,f)$ cross section are shown in Fig. 6(b).

The only earlier experimental work on the $^{209}\text{Bi}(n,f)$ cross section in the intermediate energy region was performed by Goldanski *et al.* [4]. Their data have large systematic errors due to a very wide and poorly known spectrum of incident neutrons, uncertainties in the beam monitoring, etc. Nevertheless, a qualitative agreement is seen between those and the present data [Fig. 6(b)].

Recently the $^{209}\text{Bi}(n,f)$ cross section was measured by Staples [9] in the energy region 30–500 MeV at the white neutron source at LANL using an ionization chamber as fission detector. The preliminary results agree well with the ones of the present work.

The $^{209}\text{Bi}(n,f)$ cross sections calculated with LAHET are shown in Fig. 6(b) by dashed lines with the same numbering as in Fig. 6(a). Error bars near the lines show statistical uncertainties of the Monte Carlo calculations. It is seen that the experimental data can be reproduced within a factor of about 2 by choosing an option in the LAHET code using only one of two nonequilibrium reaction stages, i.e., either intranuclear cascade (“MPM turned off”) or preequilibrium emission (“pure MPM”). On the other hand, using both nonequilibrium processes, with either the “hybrid MPM” or the “normal MPM” option, leads to an underprediction of the $^{209}\text{Bi}(n,f)$ cross section. Thus, an unexpectedly strong sensitivity of the calculated $^{209}\text{Bi}(n,f)$ cross section was found to the choice of optional modes controlling the use of the preequilibrium exciton model in the LAHET code. This large variation is surprising because LAHET reproduces double differential secondary-particle production cross sections fairly well and with a moderate parameter dependence [38]. However, one should keep in mind that the $^{209}\text{Bi}(n,f)$ cross section amounts to only 2–3 % of the total reaction cross section at these energies. On the other hand, as pointed out above, in the case of ^{238}U , where fission plays a dominant role, the LAHET code does not show a large sensitivity on the optional modes.

The solid line in Fig. 6(b) represents an evaluation of the $^{209}\text{Bi}(n,f)$ cross section by Fukahori and Pearlstein [39] in-

cluded in the High Energy File, version 6, of the US Evaluated Nuclear Data File (ENDF/B-VI) [40]. The evaluation is 20–50 % higher than the experimental data obtained in the present work. The $^{209}\text{Bi}(n,f)$ evaluation was based on an evaluation of the $^{209}\text{Bi}(p,f)$ cross section which also was made by Fukahori and Pearlstein [39] with the assumption that the $^{209}\text{Bi}(p,f)/^{209}\text{Bi}(n,f)$ cross section ratio does not depend on the incident particle energy, and is equal to 2. This assumption is not confirmed by the present experimental data. On the contrary, the present experimental data, in combination with a recent evaluation of the $^{209}\text{Bi}(p,f)$ cross section [41], show a decrease of the $(p,f)/(n,f)$ ratio from 3.6 to 2.6 with the neutron energy increasing from 73 to 162 MeV. The $(p,f)/(n,f)$ ratio calculated with the LAHET code at 100 and 160 MeV incident energies is between 3 and 5 for different options concerning the onset of the preequilibrium modes [24].

C. The $^{208}\text{Pb}(n,f)$ cross section

The present experimental data on the $^{208}\text{Pb}(n,f)$ cross section are shown in Fig. 6(c). No published experimental data are known on neutron-induced fission cross sections for separated lead isotopes in the intermediate energy region. The only previous measurements on natural lead samples, made by Reut *et al.* [5], have large systematic errors similar to those of the work of Goldanski *et al.* [4] mentioned above. Nevertheless, a qualitative agreement is seen between those and the present data.

A recent measurement of the $^{208}\text{Pb}(n,f)$ cross section in the energy region from about 50 to 500 MeV was performed by Vonach *et al.* [8] at the white neutron source at LANL using an ionization chamber as fission detector. The preliminary results are about a factor of 2–3 larger than the corresponding cross section data of the present experiment. The discrepancy tends to increase with the incident neutron energy. The reason for the discrepancy is not yet clear. The $(p,f)/(n,f)$ cross section ratio calculated from the data by Vonach *et al.* in combination with the $^{208}\text{Pb}(p,f)$ cross section evaluation by Fukahori and Pearlstein [39,40] decreases from about 1.5 at 100 MeV down to 0.6–0.7 at 500 MeV. The fact that the (n,f) cross section was found to be larger than the (p,f) cross section in the energy region of a few hundred MeV is contradictory with results from empirical studies by Perfilov [42] and Eismont *et al.* [43] in which the fission probability in the saturation region was investigated as a function of the parameter Z^2/A of the fissioning system.

Staples [9] recently made a measurement of the $^{208}\text{Pb}(n,f)$ cross section in the energy region 30–500 MeV, also at the white neutron source at LANL. The preliminary $^{208}\text{Pb}(n,f)$ cross section data of Staples are about 1.5 times larger than the $^{208}\text{Pb}(n,f)$ data reported in the present work. This relation seems to be reasonable because the lighter lead isotopes (^{206}Pb and ^{207}Pb) are expected to have larger fission cross sections than ^{208}Pb in the neutron energy region of the present work. A similar isotopic effect was found in the work by Bychenkov *et al.* [20] for proton-induced fission of lead isotopes.

The $^{208}\text{Pb}(n,f)$ cross section calculated with the LAHET code are shown in Fig. 6(c) by dashed lines with the same numbering as in Figs. 6(a) and (b). The calculation with

‘‘MPM turned off,’’ ‘‘hybrid MPM,’’ and ‘‘normal MPM’’ gave the same results as the ones given in a recent work by Prael [38]. Similar to the ^{209}Bi case, a strong sensitivity of the calculated $^{208}\text{Pb}(n,f)$ cross section was found to the choice of optional modes controlling the use of the preequilibrium exciton model in the LAHET code. The calculation with ‘‘MPM turned off’’ (default option) gives the best fit to the experimental data. It reproduces the present experimental data within about 40% for energies above about 100 MeV where the intranuclear cascade model is expected to give the most reliable results. As in the ^{209}Bi case, calculations using both nonequilibrium processes (‘‘hybrid MPM’’ and ‘‘normal MPM’’) gave an underprediction of the $^{208}\text{Pb}(n,f)$ cross section.

Prael [38] has made LAHET $^{208}\text{Pb}(n,f)$ cross section calculations using a more extensive parameter search. One can conclude from that work that the ISABEL INC model gives a slightly worse agreement with the present experimental data than the use of the Bertini INC model. The use of the Jülich level density instead of the default (Gilbert-Cameron-Ignatyuk-Cook) level density results in a strong drop of the fission cross section in discrepancy with the experimental data of the present work.

The solid line in Fig. 6(c) represents an evaluation of the $^{208}\text{Pb}(n,f)$ cross section by Fukahori and Pearlstein [39] included in the High Energy File of the US Evaluated Nuclear Data File (ENDF/B-VI) [40]. Similar to the ^{209}Bi case, the evaluation is 30–60 % higher than the experimental data obtained in the present work. The $^{208}\text{Pb}(n,f)$ evaluation was based on an evaluation of the $^{208}\text{Pb}(p,f)$ cross section which was also made by Fukahori and Pearlstein [39] and the assumption that the $^{208}\text{Pb}(p,f)/^{208}\text{Pb}(n,f)$ cross section ratio is equal to 2 and does not depend on the incident particle energy. This assumption is not confirmed by the present experimental data. On the contrary, the $(p,f)/(n,f)$ ratio obtained from the experimental data in combination with the

ENDF/B-VI High Energy File evaluation of the $^{208}\text{Pb}(p,f)$ cross section [39,40] decreases from 4.3 to 3.1 when the incident particle energy increases from 73 to 162 MeV.

VII. CONCLUSIONS

The present work gives fairly accurate experimental data on the neutron-induced fission cross sections for nuclei lighter than the actinides. The data are obtained by a nontraditional experimental technique whose applicability is confirmed by the overall agreement with other recent measurements of the ^{238}U neutron-induced fission cross section.

A significant difference is observed between proton- and neutron-induced fission cross sections both for ^{209}Bi and ^{208}Pb . The fission probability depends strongly on the charge of the fissioning nucleus in Pb-Bi-Po region and the increase of the mean charge of the fissioning nuclei caused by the incident proton results in a fission probability which is higher than for an incident neutron.

Measurements over a wider energy range would be of interest. In particular, the energy range below 70 MeV is the most suitable for extracting information on fission-neutron competition. Data at higher energies (up to 1.5 GeV) are requested for the research on accelerator-driven transmutation concepts [2].

ACKNOWLEDGMENTS

The authors are grateful to the staff of The Svedberg Laboratory for good cooperation. The targets were provided by the group of Dr. S. Solovjev, Khlopin Radium Institute. We wish to thank Dr. R. Prael for providing us with the LAHET code and Dr. Staples and Prof. Vonach for providing us with their unpublished data and for helpful remarks on the present paper. The Swedish Natural Science Research Council have financed a part of the travel costs for this project.

-
- [1] A.A. Rimski-Korsakov, Proceedings of the Specialists' Meeting on Neutron Cross Section Standards for the Energy Region above 20 MeV, Uppsala, Sweden, 1991, OECD/NEA Report NEANDC-305 'U', 1991, p. 65.
- [2] A.J. Koning, Report NEA/NSC/DOC, 1993, p. 6.
- [3] H. Condé, in *Proceedings of the International Conference on Nuclear Data for Science and Technology*, Gatlinburg, 1994 (American Nuclear Society, La Grange Park, 1994), p. 53.
- [4] V.I. Goldanski, E.Z. Tarumov, and V.S. Pen'kina, Dokl. Akad. Nauk SSSR Sov. Phys. Dokl. **101**, 1027 (1955).
- [5] A.A. Reut, G.I. Selivanov, and V.V. Yurjev, Nuclear Problem Institute report, 1950.
- [6] P.W. Lisowski, A. Gavron, W.E. Parker, J.L. Ullman, S.J. Balistrini, A.D. Carlson, O.A. Wasson, and N.W. Hill, Proceedings of the Specialists' Meeting on Neutron Cross Section Standards for the Energy Region above 20 MeV [1], p. 177.
- [7] A.V. Fomichev, I.V. Tuboltseva, A.Yu. Donets, A.B. Laptev, O.A. Shcherbakov, and G.A. Petrov, Proceedings of the International Conference on Nuclear Data for Science and Technology, Jülich, Germany, 1991 (Springer-Verlag, Berlin, 1991), p. 734.
- [8] H. Vonach, A. Pavlik, R. Nelson, and S. Wender, unpublished; H. Vonach, private communication.
- [9] P. Staples, private communication.
- [10] A.N. Smirnov and V.P. Eismont, Prib. Tekh. Éksp. [Instrum. Exp. Tech. (USSR)] **6**, 5 (1983).
- [11] A.N. Smirnov, V.P. Eismont, and A.V. Prokofyev, *Radiation Measurements*, Proceedings of the International Conference on Nuclear Tracks in Solids, Dubna, Russia, 1994 (Elsevier Science, Great Britain, 1995), Vol. 25, p. 151.
- [12] V.P. Eismont, A.V. Prokofyev, A.A. Rimski-Korsakov, A.N. Smirnov, H. Condé, K. Elmgren, S. Hultqvist, J. Nilsson, N. Olsson, E. Ramström, T. Rönnqvist and E. Tranéus, in *Proceedings of the International Conference on Nuclear Data for Science and Technology* [3], p. 360.
- [13] R.E. Prael and H. Lichtenstein, Los Alamos National Laboratory Report No. LA-UR-89-3014, 1989.
- [14] H. Condé *et al.*, Nucl. Instrum. Methods **A292**, 121 (1990).
- [15] N. Olsson, J. Blomgren, H. Condé, K. Elmgren, J. Nilsson, E. Ramström, T. Rönnqvist, R. Zorro, A. Ringbom, G. Tibell, O. Jonsson, L. Nilsson, P.-U. Renberg, and S.Y. van der Werf,

- in *Proceedings of the International Conference on Nuclear Data for Science and Technology* [3], p. 60.
- [16] R.A. Arndt, J.S. Hyslop, and L.D. Roper, *Phys. Rev. D* **35**, 128 (1987).
- [17] Scattering Analysis Interactive Dial-Up (SAID), Virginia Polytechnic Institute, Blackburg, Virginia (R.A. Arndt, private communication), version 6/21/93 of the energy-dependent VZ40 solution was used.
- [18] R.C. Byrd and W.C. Sailor, *Nucl. Instrum. Methods A* **274**, 494 (1989); S. Stamer, W. Scobel, and R.C. Byrd, in *Proceedings of the Specialists' Meeting on Neutron Cross Section Standards for the Energy Region above 20 MeV* [1], p. 154.
- [19] L. Kowalski, Ph.D. thesis, Universite de Paris, 1963.
- [20] V.S. Bychenkov, V.D. Dmitriev, A.I. Obukhov, N.A. Perfilov, and O.E. Shigaev, *Yad. Fiz.* **17**, 947 (1973) [*Sov. J. Nucl. Phys.* **17**, 496 (1973)]; **27**, 1424 (1978) [**27**, 751 (1978)]; **30**, 30 (1979) [**30**, 16 (1979)].
- [21] M. Fatyga, K. Kwiatkowski, H.J. Karwowski, L.W. Woo, and V.E. Viola, *Phys. Rev. C* **32**, 1496 (1985).
- [22] I.Yu. Gorshkov, A.T. D'yachenko, A.V. Prokofyev, A.N. Smirnov and V.P. Eismont, *Izvestija RAN, Ser. Fiz.* **57**, 178 (1993).
- [23] R.E. Prael, Los Alamos National Laboratory Report No. LA-UR-89-3347, 1989.
- [24] H. Condé, K. Elmgren, S. Hultqvist, J. Nilsson, N. Olsson, T. Rönnqvist, E. Tranéus, V.P. Eismont, A.V. Prokofyev, and A.N. Smirnov, Uppsala University Neutron Physics Report UU- NF 94/#6, 1994.
- [25] H.W. Bertini, *Phys. Rev.* **188**, 1711 (1969).
- [26] Y. Yariv and Z. Fraenkel, *Phys. Rev. C* **20**, 2227 (1979).
- [27] Y. Yariv and Z. Fraenkel, *Phys. Rev. C* **24**, 488 (1981).
- [28] K. Chen, Z. Fraenkel, G. Friedlander, J.R. Grover, J.M. Miller, and Y. Shimamoto, *Phys. Rev.* **166**, 949 (1968).
- [29] J. Barish *et al.*, "HETFIS High-Energy Nucleon-Meson Transport Code with Fission," Oak Ridge National Laboratory Report No. ORNL/TM-7882, (1981).
- [30] F. Atchison, *Targets for Neutron Beam Spallation Sources* (Kernforschungsanlage Jülich GmbH, Germany, 1980).
- [31] L. Dresner, "EVAP - A Fortran Program for Calculating the Evaporation of Various Particles from Excited Compound Nuclei," Oak Ridge National Laboratory ORNL-TM-196, (1962).
- [32] A. Gilbert and A.G.W. Cameron, *Can. J. Phys.* **43**, 1446 (1965).
- [33] A. Gilbert, F.S. Chen, and A.G.W. Cameron, *Can. J. Phys.* **43**, 1248 (1965).
- [34] A.V. Ignatyuk, G.N. Smirenkin, and A.S. Tishin, *Sov. J. Nucl. Phys.* **21**, 256 (1975).
- [35] R.E. Prael and M. Bozoian, "Adaption of the Multistage Pre-equilibrium Model for the Monte Carlo Method (I)," Los Alamos National Laboratory Report No. LA-UR-88-3238, 1988; R.E. Prael and M. Bozoian, unpublished.
- [36] P. Cloth *et al.*, "The KFA version of the High-Energy Transport Code HETC and the generalized Evaluation Code SIMPEL," Kernforschungsanlage Jülich GmbH, Report No. Jül-Spez-196, 1983.
- [37] E.D. Arthur and P.G. Young, in *Proceedings of the Conference on Fifty Years with Nuclear Fission*, Gaithersburg, 1989 (American Nuclear Society, La Grange Park, 1989), p. 931.
- [38] R.E. Prael, Los Alamos National Laboratory Report No. LA-UR-94-1817, 1994.
- [39] T. Fukahori and S. Pearlstein, in *Proceedings of the Advisory Group Meeting on Intermediate Energy Nuclear Data for Applications Organized by IAEA*, Vienna, 1990 (IAEA Nuclear Data Section, Vienna, 1991), p. 93; T. Nakagawa, T. Fukahori, S. Chiba, and Y. Kikuchi, in *Proceedings of the International Conference and Technology Exposition on Future Nuclear Systems: Emerging Fuel Cycles and Waste Disposal Options GLOBAL '93*, Seattle, 1993 (American Nuclear Society, La Grange Park, 1993), p. 467.
- [40] P.F. Rose, Brookhaven National Laboratory Report No. BNL-NCS-17541, 1991.
- [41] V.P. Eismont *et al.*, The Moscow International Scientific and Technical Centre Report No. 17, 1995.
- [42] N.A. Perfilov, *Zh. Éksp. Teor. Fiz.* **41**, 871 (1961) [*Sov. Phys. JETP* **14**, 623 (1962)].
- [43] V.P. Eismont, A.V. Prokofyev, and A.N. Smirnov, in *Proceedings of the International Conference on Nuclear Data for Science and Technology* [3], p. 397.